ESR, optical absorption, and luminescence studies of the peroxy-radical defect in topaz

Vann Priest and David L. Cowan
Department of Physics, University of Missouri–Columbia, Columbia, Missouri 65211

Hadil Yasar and Fred K. Ross
University of Missouri Research Reactor (MURR), University of Missouri–Columbia, Columbia, Missouri 65211

(Received 7 February 1991)

Fast-neutron irradiation of natural topaz crystals produces a single paramagnetic radiation damage center in high concentration. ESR of this center shows a holelike spectrum with $S=\frac{1}{2}$ and a strongly anisotropic g tensor: $g_{xx}=2.0027$, $g_{yy}=2.0055$, and $g_{zz}=2.0407$. We identify this defect as an intrinsic O_2^- center in the form of a peroxy radical. The orientation of the g tensor helps confirm this assignment, as does the extraordinary thermal stability; annealing temperatures near 800 °C are required for complete removal. Two uv absorption bands are associated with the peroxy radical, each with oscillator strength near 0.09. Pumping in the higher energy band leads to a polarization-sensitive 2.5-eV luminescence; the other uv band apparently relaxes nonradiatively.

I. INTRODUCTION

This paper describes a simple intrinsic lattice defect created when single crystals of the aluminosilicate gemstone topaz are subjected to fast neutron bombardment. The defect is shown to be an O_2^- molecule (or "superoxide") trapped at an O^{2-} site in the crystal, in the form of an RO_2^- "peroxy" radical. This defect is known to be an important one in silicates, where it was identified (in amorphous silica) by Friebele *et al.*,[1] and several recent reviews on radiation effects in silica glass describe the perioxy radical in detail.[2–4] It has also been observed in other oxides, including CaO (Ref. 5) and GeO (Ref. 6).

In the following section we present our arguments for identification of the defect. These are based on (1) the principal values of the ESR g tensor, (2) the extraordinary thermal stability under isochronal annealing, and (3) the orientation of the g tensor in the orthorhombic lattice. The simple one-electron energy-level scheme for the O_2^- that accounts for the ESR results[7] also suggests an ultraviolet absorption band and possible luminescence. uv absorption studies are described in Sec. III, and in Sec. IV, a 2.5-eV luminescent band is unambiguously tied to the peroxy radical. In the concluding Sec. V we briefly discuss a "quasimolecular" energy-level diagram for this defect that explains our ESR, optical absorption, polarization, and luminescence results.

II. IDENTIFICATION OF THE DEFECT

Topaz is a naturally occurring silicate gemstone usually found in large clear crystals, but occasionally colored by transition-metal impurities. The formula unit is $Al_2F_2(SiO_4)$, and the orthorhombic unit cell, with dimensions $a=4.64$ Å, $b=8.80$ Å, and $c=8.38$ Å, contains four formula units.[8,9] Geologically, the crystal qualifies as a *nesosilicate* because of its isolated SiO_4 structural units.

Exposure of these crystals to fast neutron bombardment[10] colors them blue and gives rise to intense anisotropic ESR signals near $g=2$, with linewidths around 10 G p-p. Subsequent 15-min isochronal anneals give the unexpected result shown in Fig. 1; the blue color (due to optical absorption at 2 eV) is not related to the ESR center. This 2-eV absorption, which we have related elsewhere to a doubly occupied dangling silicon bond,[11] will not be discussed further here. The ESR defect is surprisingly stable and only begins to anneal at temperatures above 550 °C, not far below the decomposition temperature of the crystal.[12]

The ESR pattern is determined by the symmetry of the orthorhombic *Pbnm* lattice. There are three symmetry operations:[9] (1) σ_c, a mirror plane normal to the c axis, (2) S_2, a twofold screw axis parallel to the a axis, and (3) an inversion center. When the translation of the screw is irrelevant, as it is to ESR and to the optical properties,

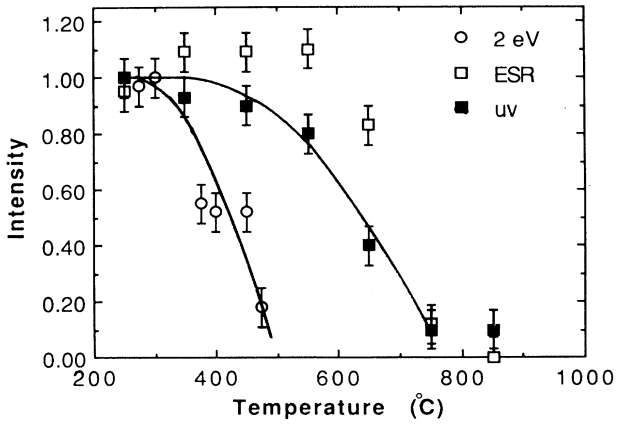

FIG. 1. Intensities at room temperature for the ESR signal and for optical absorptions in the uv and 2-eV bands, after 15-min anneals at the indicated temperature.

these symmetries reduce to three mirror planes $\sigma_a, \sigma_b, \sigma_c$ perpendicular to the lattice vectors. For any arbitrary site in the unit cell, there are then seven other equivalent sites in the cell. Since the eight orientationally distinct defects associated with a given damage center occur in four inversion-related pairs, the ESR spectrum in general consists of only four lines. The pattern will collapse to a single line whenever the magnetic field **H** is along a crystal axis. Two lines will be present when **H** is in a crystal plane.

Figure 2 shows the ESR pattern observed at room temperature in a conventiaonl X-band superheterodyne ESR spectrometer. The magnetic field is perpendicular to the b axis, 45° from the a axis, and the spectrum shows two lines of equal integrated intensity, as expected. Unresolved hyperfine interactions with nearby ^{27}Al ($I=\frac{5}{2}$) and ^{19}F ($I=\frac{1}{2}$) isotopes (both 100% abundant) are presumably the major contributors to the linewidth. Lowering the temperature does not reduce the linewidth or resolve any hyperfine splittings.

An analysis of the angular dependence then shows that all the observed lines come from a single defect with $S=\frac{1}{2}$ and a holelike g tensor given in the lattice coordinates as

$$\mathbf{g}=g_{\text{dpph}}\mathbb{1}+\begin{bmatrix}0.0049 & 0.0033 & 0.0119\\ 0.0033 & 0.0013 & 0.0046\\ 0.0119 & 0.0046 & 0.0317\end{bmatrix}, \tag{1}$$

where g_{dpph} (dpph: α,α'-diphenyl-β-picryl-hydrazyl) $=2.0037$, $\mathbb{1}$ is the identity matrix, and all off-diagonal elements can be chosen positive (the only physically meaningful algebraic sign of these terms is that of their product).

Diagonalization gives $g_{xx}=2.0027$, $g_{yy}=2.0055$, and $g_{zz}=2.0407$, and the principal axes

$$\begin{aligned}\mathbf{x}&=0.705\hat{\mathbf{a}}-0.691\hat{\mathbf{b}}-0.159\hat{\mathbf{c}}\ ,\\ \mathbf{y}&=0.608\hat{\mathbf{a}}+0.711\hat{\mathbf{b}}-0.353\hat{\mathbf{c}}\ ,\\ \mathbf{z}&=0.356\hat{\mathbf{a}}+0.152\hat{\mathbf{b}}+0.922\hat{\mathbf{c}}\ .\end{aligned} \tag{2}$$

In an oxide crystal this pattern of g values—unshifted in one direction and having large and small hole shifts in the other two directions—is diagnostic for a trapped hole in an O $2p$ orbital. Further, simple electronic rearrangements [such as an $(SiO_4)^{3-}$ cluster] would be incompatible both with the requirement for a displacive fast neutron collision to produce the defect and the extraordinarily high annealing temperature shown in Fig. 1. A model that satisfies all these conditions, though, is that of the peroxy radical, a diatomic oxygen molecular ion. This defect is one of the three major known defects in silica glass, and the most difficult to anneal. The electronic states are analogous to those for the O_2^- molecule, whose ESR spectrum was explained by Känzig and Cohen[13] and later quite exhaustively analyzed by Zeller and Känzig.[7]

Based on the one-electron energy-level diagram for the $n=2$ shell of the O_2^- molecule, as shown in Fig. 3, the g values are to first order[13]

$$\begin{aligned}g_{zz}&=g_e+2\lambda/\Delta\ ,\\ g_{xx}&=g_e\ ,\\ g_{yy}&=g_e+2\lambda/E\ .\end{aligned} \tag{3}$$

Here $g_e=2.0023$ is the free-electron g value, λ is an effective spin-orbit splitting, Δ is the $\pi_y^*-\pi_x^*$ energy separation, and E is the $\sigma-\pi_x^*$ separation. Taking $\lambda\approx 0.01$ eV gives $\Delta=0.5$ eV and $E=7$ eV.

The last remaining question is whether we can understand the principal axes given in Eq. (2). In the simple model illustrated in Fig. 3 the z axis of the g tensor lies along the O_2 molecular axis, and this feature persists in a detailed theoretical analysis of the peroxy defect in SiO_2.[14] From Eq. (2), then, the molecule is oriented with its axis nearly perpendicular to the b axis and 23° from the c axis. Pauling has suggested a very simple picture for understanding the structure of the topaz lattice;[15] the crystal is considered to be close packed in the large negative anions O and F that lie in three distinct layers A, B, and C in a double-hcp structure $ABAC\ldots$, while the small cations sit interstitially between the layers. Layer A of the unit cell is comprised of six oxygens, where the atoms are not quite coplanar because the a lattice constant is too small to accommodate them. Layers B and C are identical except for an inversion and consist of four

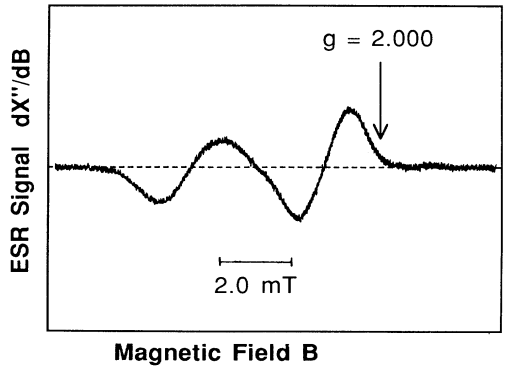

FIG. 2. ESR signal from a neutron-irradiated topaz crystal with **B** in the a-c plane, 45° from a: $T=295$ K, $f=9.3$ GHz, power is 10 μW, and modulation ≈ 0.1 mT.

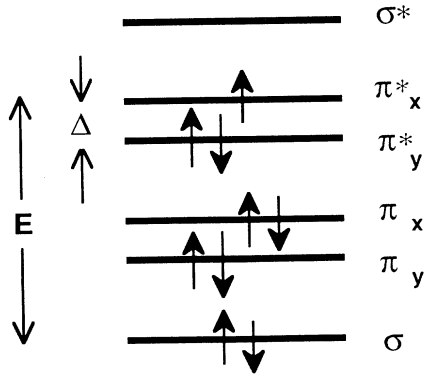

FIG. 3. The $^2\Pi_g$ ground-state configuration for the O_2^- molecule ion.

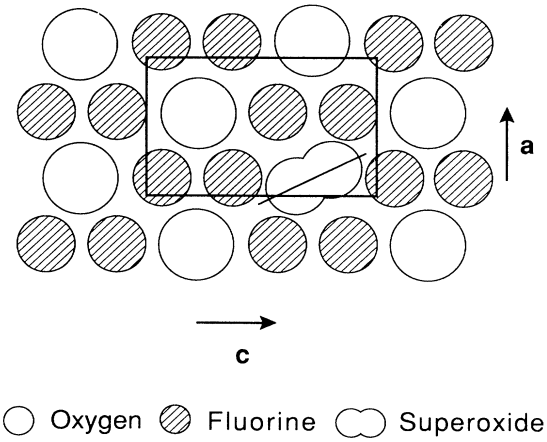

FIG. 4. The *B* layer in a nearly dhcp topaz lattice. The rectangle marks a unit cell. The superoxide (peroxy) defect is shown with its molecular axis oriented along the principal axis of the ESR *g* tensor.

fluorines and two oxygens. But these last two layers are not close packed because the ionic radius of fluorine is smaller than that of oxygen. This means an oxygen molecule can rest with a minimum of stress in the *B* (or *C*) layer. As drawn in Fig. 4, there would then be three plausible orientations for the molecular axis inside a hexagonal fluorine cage, but the cage is truly hexagonal only if the unit-cell dimension is $c/a=(3)^{1/2}$. The actual ratio in topaz is $c/a=1.806>(3)^{1/2}$, and this distortion favors the orientation shown in the figure and its mirror images. The peroxy-radical molecular axis will point, for geometric reasons, at an angle less than 30° from the *c* axis and nearly perpendicular to the *b* axis. The defect cannot sit in the *A* layer. All oxygens in the *B* and *C* layers are symmetry related, so the defect is unique, and only one of the four oxygen sites in the formula unit is available for a peroxy.

III. OPTICAL ABSORPTION STUDIES

Inspection of the simple one electron diagram shown in Fig. 3 suggests many possible excited states formed from these orbitals. In a study of O_2^- ion impurities trapped at halide sites in alkali halide crystals, Känzig found strong ultraviolet absorption bands near 5 eV and identified them in the notation of Fig. 3 as arising from $p\pi$-$p\pi^*$ transitions.[7] There are also indications in a-SiO_2 that the peroxy radical is accompanied by uv absorption, but interfering bands complicate the interpretation.[16,17]

Examination of our fast neutron damaged crystals in a Cary 14 spectrophotometer shows that the irradiation has induced a broad ultraviolet absorption band above 4 eV. Above this energy the absorbance remains almost uniformly high with no indication of structure, to the highest photon energy available, 6.2 eV. It is clear from the annealing data shown in Fig. 1 that the peroxy radical is also responsible for the uv absorption.

When the incident light is linearly polarized by a Glan-Thompson uv prism polarizer, it becomes evident that at least two absorption bands are present. For this orthorhombic crystal the polarization eigenvectors are the lattice vectors **a**, **b**, and **c**, and the polarization data are easy to interpret when both the electric field vector of the light and the propagation direction are along crystal axes. Figure 5(a) compares the absorbance of light propagating along **a** and polarized along either **b** or **c**; in Fig. 5(b) the equivalent comparison is made for light propagating along **b**. Above 4.5 eV the absorbance with **c** polarization crosses the **a** or **b** trace and becomes increasingly greater as the energy rises toward the 5-eV transmission cutoff of the prism polarizers. This crossover is not consistent with a single vibronic transition (at least within the Born-Oppenheimer approximation, where the polarization is determined by the invariant electronic part of a vibronic wave function) and we can tentatively assume two separate absorption bands arising from the same defect.

The transition responsible for the higher of these two bands can be identified. The $^2p\pi\rightarrow{}^2p\pi^*$ transition mentioned in the beginning of this section was the only uv absorption observed by Känzig in substitutional O_2^- impurities, and is the dominant absorption for the O_2^- molecule.[18] This allowed electric dipole transition has a transition dipole oriented along the molecular axis (see below). Since the molecular axis (z) of the peroxy in topaz is only 23° from the *c* axis, even after summing over the eight symmetry-related orientations there is a strong anisotropy, and light polarized along the *c* axis will give by far the strongest absorbtance into this transition. The higher of our two bands satisfies this selection rule.

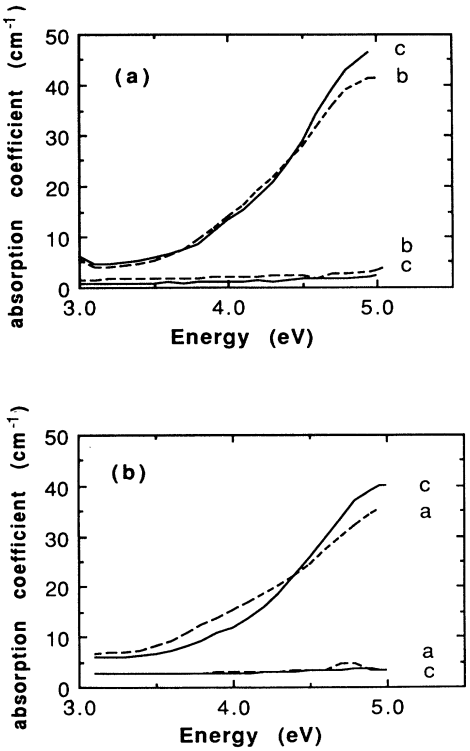

FIG. 5. uv absorption in neutron damaged (upper curves) and undamaged (lower curves) topaz (a) when the electric field vector of the light is along the *b* or *c* axis and (b) the electric field vector is along *a* or *c*.

Smakula's formula[19] allows a calculation of the oscillator strength f:

$$f=(1.29\times10^{17})\frac{n\alpha W}{N(n^2+2)^2}\ , \tag{4}$$

where N is the defect concentration (cm^{-3}), n is the index of refraction, α is the peak height (cm^{-1}), and W is the full width at half maximum (FWHM) (eV). In one sample we measured 4.9×10^{18} spins/cm^3 and an optical density of $\alpha=35\ cm^{-1}$ at 5 eV. Using a FWHM of approximately 1.4 eV leads to an oscillator strength of 0.09.

The quantum theory of radiation gives for the oscillator strength f

$$f=\frac{8\pi^2}{3}\frac{m\nu}{he^2}|\langle m|\mathbf{d}|n\rangle|^2\ , \tag{5}$$

where $\langle m|\mathbf{d}|n\rangle$ is the matrix element for an electric dipole transition between states m and n, ν is the frequency (Hz), m is the electron's mass (kg), h is Planck's constant (J s), and e is the elementary charge. For the ${}^2p\pi\rightarrow{}^2p\pi^*$ transition, $\langle m|\mathbf{d}|n\rangle=eR/2$, where R is the nuclear separation. For molecular oxygen, $R=1.3$ Å, and therefore $f=0.19$, in satisfactory agreement with the rough experimental value of 0.09.

IV. LUMINESCENCE STUDIES

There are no published reports of luminescence from peroxy-radical defects in crystals, but the O_2^- impurity has long been known to produce visible luminescence[7] when pumped in the $p\pi\rightarrow p\pi^*$ absorption band. Since we had observed an uv absorption in the peroxy radical with all the characteristics of this O_2^- band, we were motivated to look for the analogous luminescence.

Our experimental setup consisted of a 1000-W xenon lamp, a split quartz prism and a Bausch and Lomb monochromator, a liquid-nitrogen Dewer with quartz windows and a cold finger as a sample mount, an optical chopper, a Perkin-Elmer monochromator as an analyzer, various photomultiplier tubes, and a lock-in amplifier. When pumped with uv light, all topaz samples containing peroxy-radical defects showed a very weak luminescence that was nonetheless clearly visible as a blue-grey glow to the dark-adapted eye. The spectrum of this luminescence is shown in Fig. 6; the peak intensity is near 490 nm and the band has a FWHM of 0.55 eV. At liquid-nitrogen temperature the peak emission is about three to five times greater than at room temperature. We were not able to directly correlate the luminescence intensity with the peroxy-radical concentration because all our radiation-damaged samples were optically thick in the uv.

As a brief aside, one also observes the luminescence when the sample is pumped by high-energy electrons. These electrons, with energies of order 15 keV, were generated photoelectrically when molybdenum x rays from a commercial tube struck the topaz. Once again, the blue-grey luminescence was visible to the eye. It was estimated to be somewhat stronger than before, but no attempt was made to quantitatively analyze this experiment.

A rough measure of the quantum efficiency for luminescence as a function of the incident photon energy is shown in Fig. 7. These data were obtained by comparing at each wavelength the emission of the topaz with that of a reference ZnS phosphor mounted in the same geometry, and assuming a quantum efficiency for the ZnS of unity at high energy. The slight decline in the ZnS efficiency as the band gap is approached is as expected. Contrast this with the dramatic fall off in the topaz's efficiency. At the shortest pumping wavelengths the quantum efficiency is not all that far below that of the ZnS standard, but at 4 eV the efficiency has fallen 3 orders of magnitude, even though the sample is still optically thick in the uv absorption band.

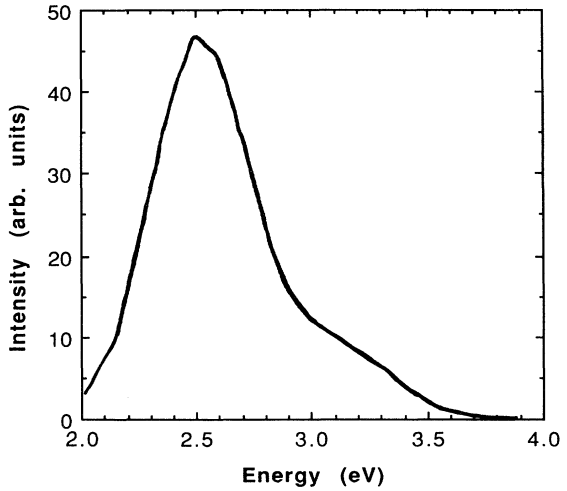

FIG. 6. Luminescence spectrum at 77 K of a neutron-damaged topaz. The sample is optically pumped with 4.5-eV light.

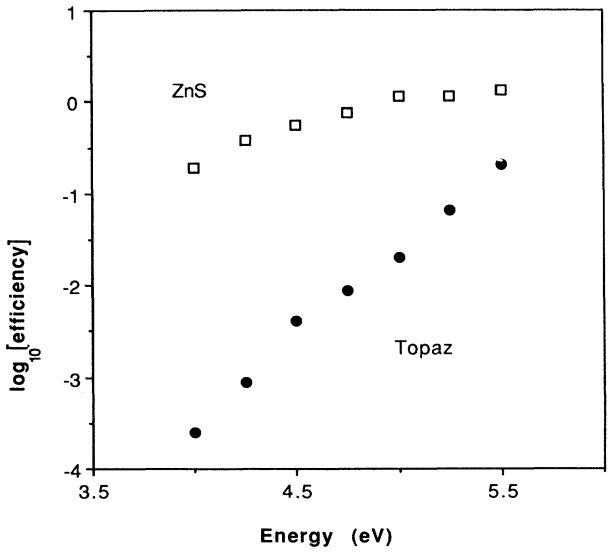

FIG. 7. Relative quantum efficiencies for luminescence for a ZnS phosphor (open squares) and a neutron-damaged topaz crystal (closed circles) as a function of the photon energy of the pumping light.

The rapid variation of quantum efficiency with pumping wavelength has a natural interpretation in view of the composite optical absorption described in the previous section. If the luminescence is only due to the *upper* of the two uv bands, and the lower band is completely nonradiative, then the quantum efficiency will just reflect the fraction of pump light absorbed in the upper level. The polarization-sensitive optical absorption shown in Fig. 5 suggests that at an incident photon energy of 5 eV only about 10% of the absorption is into the upper band, consistent with the quantum efficiency of a few percent. If we model the absorption by two overlapping but displaced Gaussians, the linear variation in log quantum efficiency with energy then follows immediately.

Presumably the upper band is the luminescent $p\pi$-$p\pi^*$ transition described by Känzig for the trapped O_2^- molecule.[7] We can test this conjecture, and other features of our interpretation, by using the polarization selection rules. The $p\pi$-$p\pi^*$ transition will be driven with a transition dipole parallel to the molecular axis z, which is not far from the crystal axis c. Because only a small fraction of the incident photons are absorbed into this upper band, any polarization-sensitive increase in optical absorption strength will be reflected in increased luminescence. In particular, orienting the **E** vector of the pump light along the c axis should cause the fraction of light absorbed into the upper band to be greater than that with **E** perpendicular to the c axis by a factor of order $\cot^2(\theta_c)=5.6$, where θ_c is the 23° angle between the z and c.

This effect has been observed. Figure 8 shows the results obtained by linearly polarizing the incident pump light with a Glan-Thompson prism polarizer. The geometry of our experimental set up prevents us from directly comparing a, b, and c axes of polarization, but the luminescence occurring when **E** is parallel to the c axis [Fig. 8(a)] can be contrasted to that when **E** is perpendicular to the c axis [Fig. 8(b)]. A comparison of the intensities (at 4.5 eV, where the optical absorption is almost completely isotropic) indicates that the fraction of light absorbed into the higher-energy band is roughly a factor of 5 greater when **E** is parallel to the c axis, and we consider this to be a fairly striking confirmation of our picture.

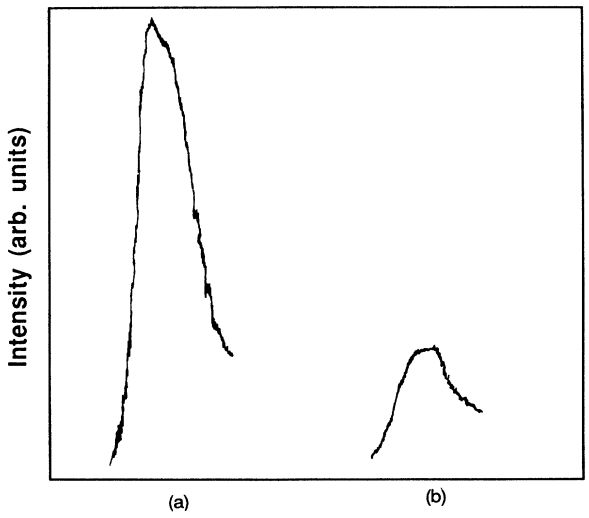

FIG. 8. Luminescent intensities at 77 K (a) when the 4.5-eV pump light is linearly polarized along c and (b) when the pump light is linearly polarized perpendicular to c.

V. DISCUSSION

All of the experimental results described in the previous sections can be summarized with the help of the level diagram shown in Fig. 9. This diagram is just, with one exception, the many-electron version of Fig. 3. It represents the low-lying energy levels of the O_2^- molecule classified according to the symmetry group D_{∞_h}. These free O_2^- levels have been studied numerically by Krauss *et al.*,[20] who conclude that at internuclear separations less than 3.0 a.u. (the bond length for free O_2^- is 1.3 Å or 2.5 a.u.), only two Π and two Σ states are low enough in energy to play any role, and these four states appear in the same order and with about the same energy as in Fig. 9. We have no experimental information about the $^4\Sigma_u$, which has no first-order influence on the g tensor, and is optically forbidden (by the change in spin) to order $(\lambda/\delta E)^2\approx 10^{-4}$. In Sec. II we estimated the $^2\Sigma_g$ to be around 7 eV above $^2\Pi_g$ from the measured ESR g_{yy}, and the $^2\Pi_u$ is just our luminescent $p\pi$-$p\pi^*$ level. We also require a lifting of the axial degeneracy in the $^2\Pi_g$ by about 0.5 eV to account for g_{zz}.

A simplest best fit to the optical absorption in the ultraviolet leads to two Gaussians, each of width 1.4 eV (FWHM), centered at 5.2 and 6.2 eV, and this decomposition produces very satisfactory agreement with both the polarization data of Fig. 5 and the luminescence data of Fig. 7. The 6.2-eV level is the $^2\Pi_u$, leaving only the state "?" at around 5.2 eV without a natural interpretation. We do know it has a large electric dipole oscillator strength, shows no strong selectivity with polarization,

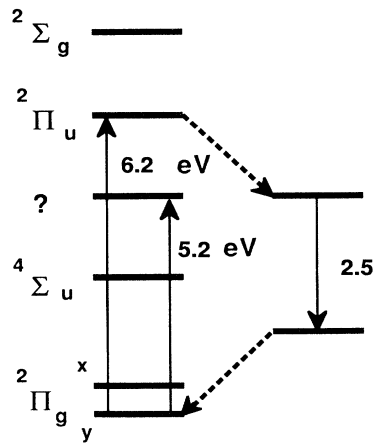

FIG. 9. A proposed molecular-energy-level diagram for the peroxy-radical defect. This diagram is nearly identical to that for an O_2^- molecule, except for the addition of one unidentified nonradiative state. The energies attributed to the absorptions are best-fit values.

and is nonradiative. We believe even this anomalous 5.2-eV state is easily rationalized in terms of molecular orbitals. The last electronic levels to be filled in O_2^- are *antibonding* levels, and a glance at Fig. 3 shows that all the excited-state configurations that can be reached optically have as much or more antibonding character. Some of these levels will fall drastically in energy as charge is removed from between the atoms by binding into a peroxy, or with covalency. A nice example is provided by the molecule methyl peroxide,[21] H_3CO-OH, which has *dissociative* optically accessible excited states at low energy whose character is closely analogous to that of the excited states of O_2^-. It seems very likely that a configuration which is dissociative in the molecule would be nonradiative in a solid, and that the level we see at 5.2 eV corresponds to one of these states.

Aside from lowering the energy of those excited states with strong antibonding character, the net effect of bonding the O_2 into a peroxy radical is probably small. For instance instead of *gerade* and *ungerade* the atomic p orbitals now form "in phase" and "out of phase" hybrids, but the bonding-antibonding distinction persists.[21] A much more fundamental question is why it makes any sense at all to describe a solid-state defect with a free-molecule energy-level diagram. The calculations of Edwards and Fowler[14] provide a very limited justification (in the notation of Fig. 9 they showed a $^2\Pi_{gx}$-like state lying just above the $^2\Pi_{gy}$-like ground state). The somewhat more extensive consistency we find there is, at least to us, something of a mystery.

ACKNOWLEDGMENTS

We would like to thank Professor E. B. Hensley for his help with the luminescence studies, and for several useful discussions. This work was supported in part by internal funding from MURR and by a grant from the Army Research Office.

[1]E. J. Friebele, D. L. Griscom, M. Stapelbroek, and R. A. Weeks, Phys. Rev. Lett. **42**, 1346 (1979).
[2]D. L. Griscom, in *Radiation Effects in Insulators,* edited by J. A. Davies, D. A. Thompson, and G. Zubauskas (North-Holland, Amsterdam, 1990), pp. 12–17.
[3]D. L. Griscom, in *Defects in Glasses,* edited by F. L. Galeener, D. L. Griscom, and M. J. Weber (Materials Research Society, Pittsburgh, 1986), Vol. 61, pp. 213–221.
[4]D. L. Griscom, J. Non-Cryst. Solids **73**, 51 (1985).
[5]T. P. P. Hall, J. Phys. C **8**, 1921 (1975).
[6]L. A. Kappers, O. R. Gilliam, and M. Stapelbroek, Phys. Rev. B **17**, 4199 (1978).
[7]H. R. Zeller and W. Känzig, Helv. Phys. Acta **49**, 845 (1967).
[8]L. Pauling, Proc. Natl. Acad. Sci. U.S.A. **14**, 603 (1928).
[9]P. H. Ribbe and G. V. Gibbs, Amer. Mineral. **56**, 24 (1971).
[10]The topaz crystals were bombarded at the University of Missouri Research Reactor (MURR) at a standard irradiation site. Typical neutron fluences were of the order of 10^{18} fast neutrons (1 MeV equivalent) cm^{-3}.
[11]V. Priest, D. L. Cowan, D. G. Reichel, and F. K. Ross, J. Appl. Phys. **68**, 3035 (1990).
[12]H. Saito and M. Ushio, J. Ceram. Assoc. Jpn. **76**, 412 (1968).
[13]W. Känzig and M. H. Cohen, Phys. Rev. Lett. **3**, 509 (1959).
[14]A. H. Edwards and W. B. Fowler, Phys. Rev. B **26**, 6649 (1982).
[15]L. Pauling, *The Nature of the Chemical Bond* (Cornell University Press, Ithaca, 1960).
[16]E. P. O'Reilly and J. Robertson, Phys. Rev. B **27**, 3780 (1983).
[17]E. J. Friebele, P. L. Higby, and T. E. Tsai, Diffus. Defect Data **53-54**, 203 (1987).
[18]H. S. W. Massey, *Negative Ions* (Cambridge University Press, Cambridge, 1976), p. 190.
[19]A. Smakula, Z. Phys. **59**, 603 (1930).
[20]M. Krauss, D. Neumann, A. C. Wahl, G. Das, and W. Zemke, Phys. Rev. A **7**, 69 (1973).
[21]J. Michl and V. Bonacic-Koutecky, *Electronic Aspects of Organic Photochemistry* (Wiley-Interscience, New York, 1990), p. 382.